A NEW, EARTH-BASED RADAR TECHNIQUE FOR THE MEASUREMENT OF LUNAR TOPOGRAPHY

S. H. ZISK
Haystack Observatory, Westford, Mass., U.S.A.

Abstract. Radio interferometry is a new technique for the measurement of the surface topography of the Moon. Elevation data may be obtained directly without regard for unambiguously-identified features, for any lunar surface element that yields a recognizable radar echo.

A program has been undertaken at the Haystack Observatory for the topographic mapping of the major part of the lunar Earthside hemisphere. Some results are presented for the Alphonsus-Arzachel region, showing evidence for a late lava flow of a viscosity and, hence, presumably a chemical composition, differing from that of near-by mare surfaces.

1. Introduction

The radar reflective properties of the lunar surface have been measured with high resolution by several investigators over the past few years. (Pettengill and Thompson, 1968; Thompson *et al.*, 1970; Zisk *et al.*, 1971). The most detailed measurements are made using the so-called delay-doppler method of resolution, where the echo signal is analyzed simultaneously in both time-delay and doppler frequency shift with respect to the transmitted waveform. This method of resolution results in a two-dimensional plane projection of the lunar surface reflectivity, analogous to an optical photograph, which can then be re-projected into any of the standard cartographic projections by the use of techniques common to optical photography of the Moon. As is explained below, the radar maps are not projections along the Earth-Moon line-of-sight like an optical photograph, but rather along a perpendicular to the line-of-sight, nearly parallel to the apparent rotation axis.

The original two-dimensional radar maps yielded much valuable information about the physical nature of the lunar surface, e.g., relative frequency of rocks on the scale of the wavelength, mean slopes, mean dielectric constant or porosity. Information about topographic relief of the surface can also be obtained by any of several elaborations of the radar mapping technique. In this paper we shall discuss some results from a program at Haystack Observatory to map the topography of the Earthside lunar hemisphere by one such method, that of radar interferometry. This method appears to be the most efficient and accurate alternative of those we have so far considered, and will be described in detail.

The radar interferometer measurement of topography is best explained as an extension of the earlier two-dimensional delay-doppler technique. I shall therefore first review this technique and mention briefly several of the alternative methods for measuring the third dimension.

Communication presented at the Conference on Lunar Geophysics, held between October 18–21, 1971, at the Lunar Science Institute in Houston, Texas, U.S.A.

2. Measurements

The Haystack planetary 'radar' telescope radiates a monochromatic signal at 7840-MHz frequency (about 3.8 cm wavelength). For the lunar observations, the signal is emitted in a brief pulse of from 3 to 13 μs duration in order that the elapsed round-trip time for the echo can be related accurately to the location of the reflecting spot on the lunar surface.

As can be seen from Figure 1, the round-trip time delay of the echo determines the location of the reflecting area to within an annulus centered on the vector line-of-sight from the radar to the lunar center. This provides one dimension of fine-grain resolution (typically less than 1 km) within the overall beam of the radar, which projects a circle of about 400 km diam at lunar distance.

Independent resolution of the lunar echo in another direction is accomplished by frequency-analyzing the doppler shift of the echo resulting from the apparent lunar motion. The apparent radial and angular velocities of the Moon each have two components: the true orbital motions, including the forced physical librations; and the diurnal rotation of the Earth.

The apparent radial velocity consists mainly of a sinusoidal component due to diurnal rotation of the Earth. At the Haystack frequency of 7840-GHz, the total doppler shift at the lunar subradar point* varies typically from +16 kHz at moonrise to −16 kHz

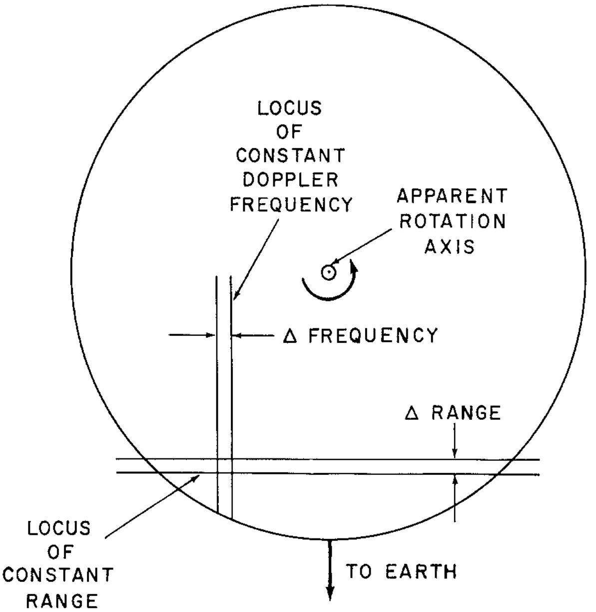

Fig. 1. Schematic of the two-dimensional fine-grain resolution of a lunar radar echo by delay and doppler analysis.

* The *subradar point* is the point on the lunar surface pierced by the line-of-sight from the radar to the lunar center of mass.

at moonset. Only near transit (and hence near zero doppler) is the orbital motion of the Moon a significant factor.

The apparent angular velocity vector, however, is the cross-product of two vectors: (1) The vector line-of-sight from the radar to the lunar subradar point, and (2) the vector sum of the velocities of the radar-site and of the lunar surface at the subradar point. Of the two latter velocities, that of the radar site is the greater by at least an order of magnitude. As a result, the apparent angular velocity vector when the Moon is in northern declinations will be directed toward the eastern limb at moonrise, toward the western limb at moonset, and toward the north pole near transit. This represents a range of position angles over 180°, which in principle enables every area on the Earth-side hemisphere to be observed at some time when it is near the doppler axis*. As can be seen from Figure 1, this is the orientation for optimum two-dimensional resolution. When the Moon is in southerly declinations, the doppler axis ranges similarly over more than 180°, from west through north to east. The extremes of this range, however, are not visible from Haystack because of its northern latitude. There are modifications to this general situation when the lunar declination is changing rapidly near zero declination, and the apparent lunar motion is then a more significant factor.

The doppler component resulting from the apparent lunar angular velocity is proportional to the distance between the surface element in question and the doppler axis, as described below. Typically, this doppler component increases from zero at the subradar point to between 30 and 100 Hz at the limb. It seldom exceeds 150 Hz, and occasionally drops to 10 Hz or below. At the largest and smallest values, useful data are difficult to obtain because of limitations of the equipment.

To facilitate the description of the radar topography measurements technique, we first define the usual radar coordinate system centered on the lunar center-of-mass. The z-axis is directed toward the radar; the y-axis along the doppler axis as defined above; and the x-axis, to make up a right-handed orthogonal system, in the direction of decreasing doppler-frequency. The radar signal received at time t represents the integral of the echo from points in an annulus at constant z, given by

$$z = R_0 - tc/2, \tag{1}$$

where R_0 is the distance from the radar to the lunar center of mass; t is the observed time of the echo after the transmission of the pulse; and c is the velocity of light. There is some lack of rigor in the present discussion, but it is sufficiently precise to explain the general method.

The x-coordinate of the resolved backscattering element is obtained by frequency-analysis of the echo. As mentioned above, there is a gross doppler shift, f_0, in the reflected signal due to the relative velocity between the lunar center of mass and the radar. In addition, the apparent rotation of the Moon imports a secondary Doppler shift, f_D, that increases linearly with distance from the rotation axis, i.e., with $(-x)$.

* The *doppler axis* is the component of the apparent angular velocity vector that is perpendicular to the line-of-sight from the radar to the lunar center of mass.

Then the total doppler shift is

$$f_0 + f_D = \frac{-2\dot{R}_0 - 2\Omega x}{\lambda}, \tag{2}$$

where Ω is the apparent angular velocity of the Moon, λ is the wavelength of the transmitted radiation, and $\dot{R}_0$ is the velocity of the lunar center of mass with respect to the radar. As is shown in Figure 1, the radar signal within a given doppler frequency band represents the integral of the echo from the points of the annulus at constant x. It follows that

$$x = -\frac{f_D \lambda}{2\Omega}. \tag{3}$$

The position of the backscattering element on the lunar surface can now be located at the intersection of two annuli, with a precision determined by the time and frequency resolution of the radar. These are about 3 μs and 0.04 Hz for the Haystack radar, equivalent to 450 m and about 1 km respectively at the Moon.

The shape of the two resolution strips is circular only for an exactly-spherical Moon. Figure 2 demonstrates the more general shape of the resolution cell. Here, the time and frequency resolution each defines its plane of non-zero thickness ('slab') perpendicular to the z- and x-axis respectively. The intersection of these two 'slabs' defines the most general resolution cell, whose position is fixed in two dimensions by the observed time-delay and frequency offset, but is unbounded in the third. It has thus the form of

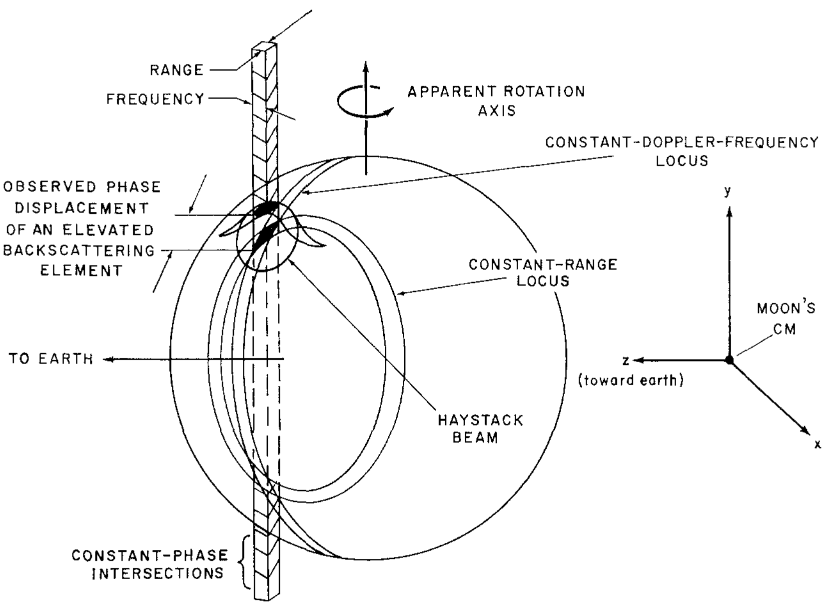

Fig. 2. Perspective view of the delay-Doppler diagram of Figure 1, showing the fundamental radar resolution cell or 'stick' in three dimensions.

a 'stick' parallel to the y-axis. The problem of radar measurement of the topography is thus equivalent to finding the y-coordinate of the backscattering element along the resolution 'stick'.

3. Alternative Methods

In earlier measurements of radar backscattering strength, there was no independent information on the location of the backscattering surface elements along the resolution-stick of Figure 2. We assumed, therefore, a spherical lunar surface, and re-mapped the measurements from their fundamental delay-doppler projection into a standard cartographic projection (Mercator or Lambert Conformal). Features in the resulting maps that are not actually located on the sphere at 1738 km radius are displaced by an amount d, in the great-circle direction away from the nearest Doppler pole (Figure 3). The magnitude of the displacement is

$$d = h \tan \phi , \tag{4}$$

where h is the true elevation above the sphere and ϕ is the angle between the local vertical and the doppler axis.

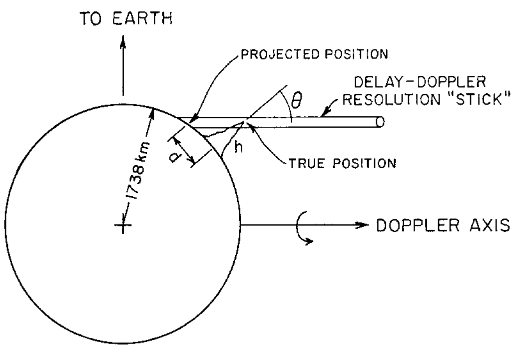

Fig. 3. Displacement of an elevated feature in a two-dimensional delay-Doppler radar map as a result of a parallax.

This parallax effect can be used to measure surface topography by a method analogous to stereo-photogrammetry*. Since radar observations are generally made at varying lunar librations, on two overlapping observations a given elevated feature would be displaced by different amounts depending on the libration geometry and the elevation above a reference sphere. This effect could be used to determine lunar elevations from a series of radar measurements. Optical photography has been so used for many years. Kopal (1968) has reported the most recent and probably most accurate work, and also includes an excellent bibliography. See also Kopal (1966) for a good analysis of the method. The usual difficulties with the optical measurements would

* The photogrammetry method for radar measurement of lunar topography was worked out jointly by T. W. Thompson and S. H. Zisk in 1969, and independently by I. I. Shapiro about a year earlier unbeknownst to us.

also apply to radar stereogrammetry: the problem in identifying precisely the same point of the lunar surface on two maps, and the error resulting from any uncertainty in the predictions of the lunar librations. There would be an improvement in the accuracy of the radar measurement, on the other hand, because of the large available range of libration angles, compared with Earth-based optical librations of no more than about $\pm 8°$.

Of the several other possibilities for topography measurement, one of the more promising is a hybrid of radar and optical parallax measurements*. If the same feature can be identified precisely on both an optical and a radar the two viewing angles will be nearly 90° apart, giving an optimum parallax geometry. In addition, the effect of libration prediction errors would be reduced by a factor of $\sqrt{2}$ if both measurements were made simultaneously.

4. Interferometry

The most promising method of all, however, appears to be radar interferometry. The results presented later in this paper were produced with the Haystack-Westford interferometer to be described below (Rogers and Ingalls, 1970); none of the alternative techniques has yet been found necessary.

Perhaps the strongest argument for interferometry (and the one that is virtually unique) is that measurements are not restricted to identifiable features. The elevation of any surface element that gives a measurable radar echo can be obtained, since the result of the measurement is a set of y-coordinates of all the resolved elements of a radar backscatter map. In the present case, resolution along the delay-doppler 'stick' is accomplished by use of a radar interferometer, comprising the 36 m diam Haystack radar which illuminates the Moon at a frequency of 7840-MHz and also serves as one element of the interferometer receiver together with the 18 m diam Westford Communications antenna located about 1200 m to the south, which serves as the other element. Figure 4 is a block diagram of the interferometer and datarecording systems. The echo signals from the moon are recorded at both Haystack and Westford, and are processed separately into delay-doppler maps.

Considering a given lunar surface element that appears in a pair of corresponding resolution cells on the Haystack and Westford maps we see that the phase difference between the two signals depends only upon the location of this element in the fringe pattern of the interferometer (Bracewell, 1962). The interferometer has its greatest resolving power in a direction along the projection of its baseline. Thus, the position of a lunar surface-element along its resolution stick can be determined from the measured phase-difference between its two resolved echo signals at Haystack and Westford, as long as there is a non-zero component of the projected interferometer baseline along the resolution stick.

For a given accuracy $\Delta\phi$ in the phase measurement, the spatial resolution in the

* Many of the possible alternative methods for topography measurement were suggested originally by I. I. Shapiro. T. W. Thompson first recognized the value of the Haystack-Westford interferometer for this work.

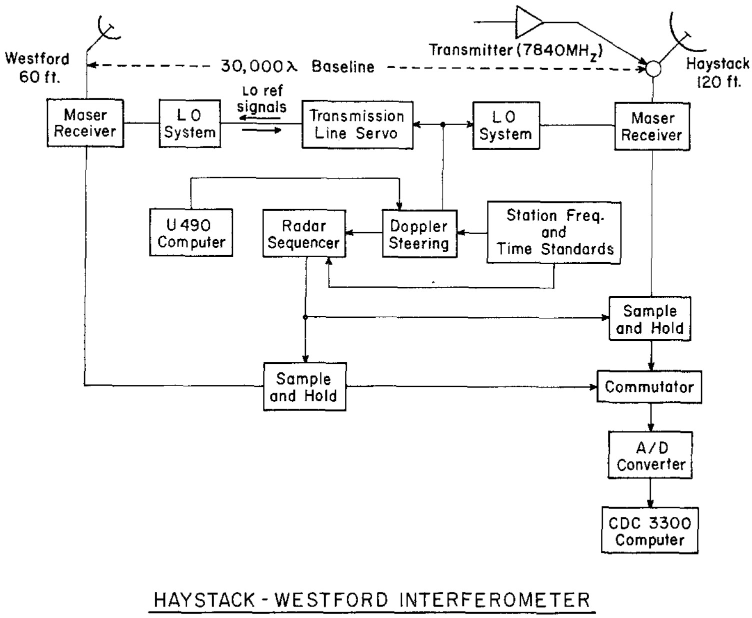

Fig. 4. Block diagram of the Haystack-Westford Radar Interferometer.

y-direction, Δy, depends on the fringe spacing, d (defined as the distance between adjacent zero-phase-difference lines at the Moon), and the fringe angle, p (defined as the angle between the projected baseline and the resolution stick) by

$$\Delta y = \frac{d \Delta \phi}{2\pi \cos p}. \tag{5}$$

For the present interferometer, d varies between 10 and 20 km during useful observing periods, and $\Delta\phi$ is less than 0.16 rad during the winter, when atmospheric seeing is excellent. The typical y-resolution is then

$$\Delta y = \frac{0.3}{\cos p} \text{ km}. \tag{6}$$

If we are willing to accept an uncertainty of 500 m in y, then p may vary by $\pm 45°$, a criterion which is satisfied at least 75% of the time the Moon is above the horizon at Haystack.

The concept of x or z accuracy, on the other hand, is somewhat less straightforward. Although one resolution element covers an area of several km^2, the elevation measurement nevertheless represents a precise weighted mean over the entire resolution element, rather than a fixed height whose location has such an uncertainty. The weighting function is the relative echoing strength of various features within the element. Therefore, the calculated height will not always correspond to the center of the resolved area, but will be biased toward Earth-facing slopes. One peculiar effect of this bias is that a mountain peak will generally be measured as lower than its true peak elevation, and a narrow valley as shallower than its greatest depth. The only exceptions should be those unlikely features that are topped (or bottomed) by a plateau comparable in area with the resolution element, i.e., $\approx 1 \times 2$ km.

In the course of an observation, the limits on the x and z dimensions of a resolution cell are set by pragmatic considerations. Because of the need to prevent frequency-aliasing in the processing of the time-sampled echo signal, the width of the complete map in the x (= Doppler-frequency) direction is set, by adjustment of the radar pulse interval, approximately equal to the diameter of the Haystack beam, or about 450 km at the distance of the Moon. The x-dimension of the resolution element (see Figure 1) is then simply a given fraction of this length, which is set by the present data-processing parameters to be $\frac{1}{256}$. Finer resolution by as much as a factor of four is probably feasible, but adds to the time and complexity of the data processing.

Resolution in the z-direction is similarly a function of the observation and data-processing parameters. The minimum interval between successive range boxes is 3 μs, corresponding to a distance of 450 m. This interval is set by the speed of the computer interface equipment. However, we use this narrow 3-μs resolution only for the central part of the lunar disk, where the projected surface resolution would otherwise be greatly degraded. On other areas further from the center, the z-resolution is intentionally increased by lenghtening the transmitted pulse. The goal for the present program is to maintain a z-resolution projected on the lunar surface of about 1 km. Later measurements of selected smaller parts of the Earthside hemisphere will be carried out with higher resolutions, as may be suggested by the analysis of preliminary results.

5. Results

Figures 5 and 6 are maps of the phase and magnitude of the interferometer signal over the region including the craters Alphonsus and Arzachel. This area was the first to be examined in any detail, and the results of the examination, including several duplicate sets of independent measurements yielding consistent results, have appeared in an internal report (Haystack Observatory, 1971). Note that the area to the west of the craters (centered at about 9° W, 12° S) is a part of Mare Nubium. The radar elevation contours show this part of the Mare to have a level floor (less than 300 m tilt over a 150 km north-south span). While a combination of errors might lead to an apparently constant elevation, it is not very likely, and the level topography does in fact lend confidence to the measurements.

The floors of Alphonsus (2°W, 13°S) and Arzachel (1.5°W, 18° S) are also level in the north, but each shows a gradual upward slope in the southern half extending from the east-west diameter toward the south rim, and centered on a SE-trending radial ridge. The two ridges are aligned with each other, with one of the straight sections of the rim of Ptolemaeus, and with the center of Mare Imbrium, and may thus represent a flow of viscous lava through faults remaining from the Imbrium event. In this case, since the ridge flow is clearly more recent than the smooth flows making up the remain-

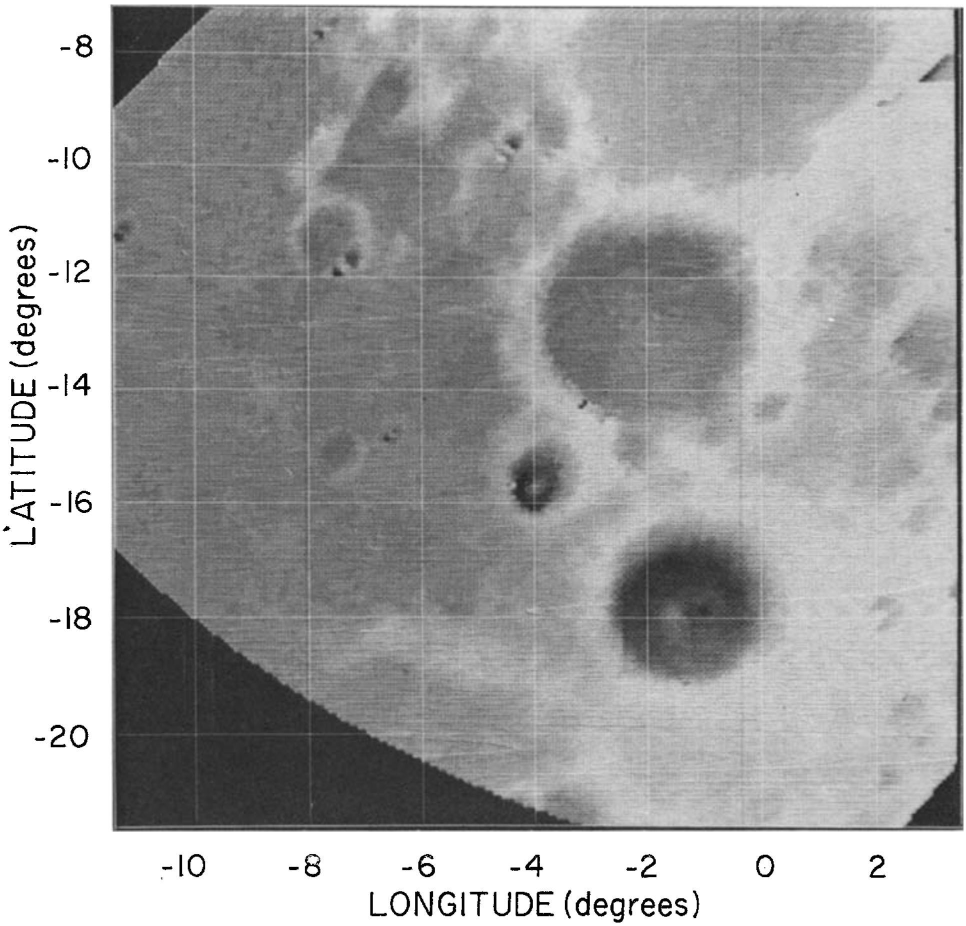

Fig. 5. Phase of the interferometer signal from the Alphonsus region. Alphonsus and Arzachel are located at (2° W, 13° S) and (1.5° W, 18° S). Black to white on this map represents a range of 360° of phase, which equals about 5 km difference in elevation at this angle of incidence (see Figure 3).

ing level floor, it may represent the last pool of cooling anorthositic lava exuded from beneath this area.

In the northern part of the map there appears a portion of the crater Ptolemaeus. This crater was recently observed from Apollo orbit, to have a small negative gravitational anomaly (Sjogren *et al.*, 1971). The floor of Ptolemaeus, is however, not only at a greater elevation than the above mentioned craters, but also probably greater by 200–300 m than the floor of Mare Nubium to the west, which does not appear to have an associated gravitational anomaly (Muller and Sjogren, 1968). One conclusion from these facts is that the floor of Ptolemaeus either consits of rock with a chemical composition of low density (e.g., anorthositic), or is underlain by a relatively thick, porous, regolith layer that may have originated in brecciated material that slumped from the crater walls.

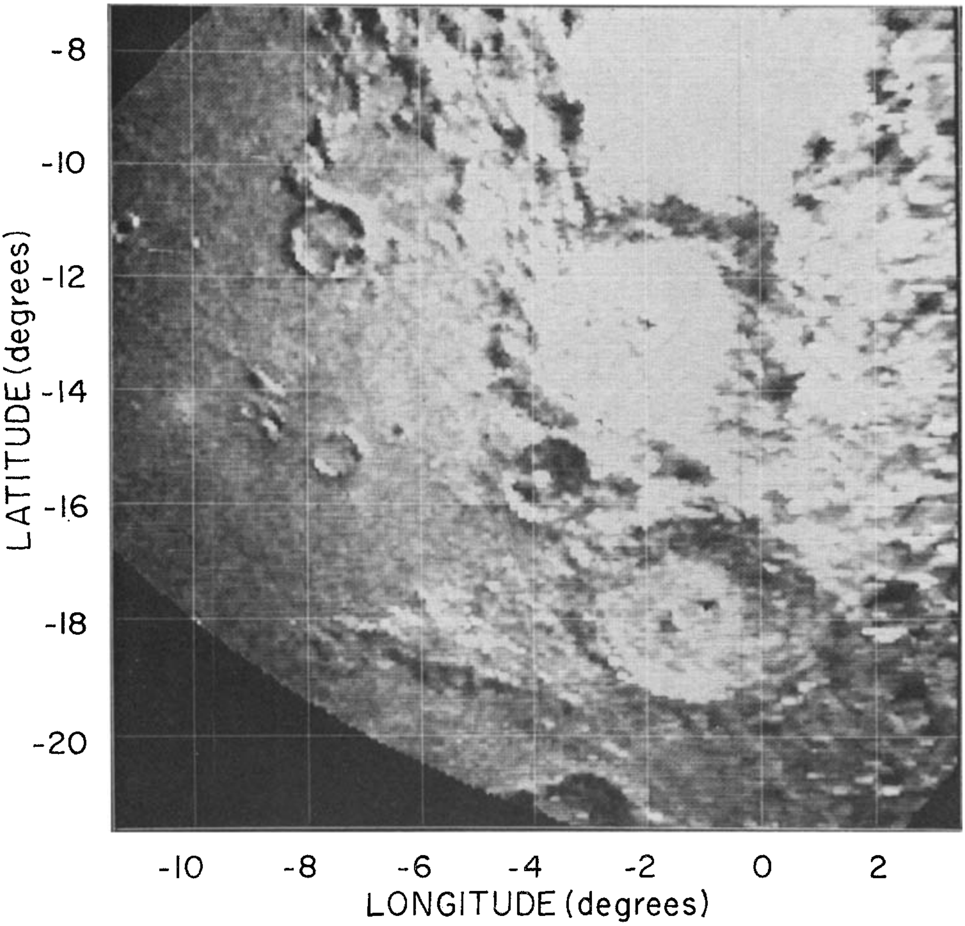

Fig. 6. Magnitude of the interferometer signal for the same observation as Figure 4. Lighter shading represents increased radar backscatter.

Acknowledgements

Thanks are due to many members of the Haystack Observatory staff for assistance with the observations and their processing. Alan E.E. Rogers rendered extremely valuable assistance with the interferometer and the early computer programming. R.P. Ingalls and J.I. Levine built or adapted most of the timing, pre-processing and data-handling parts of the interferometer receiver. G.W. Catuna kept order among the many reels of 'raw' and partly-processed data that formed the milestones toward the finished maps. Thanks are also due to G.H. Pettengill and T.R. McGetchin of MIT Earth and Planetary Science Department for valuable and stimulating discussions.

The work reported here was funded primarily by NASA Manned Spacecraft Center under contract NAS9-7830. Haystack Observatory is operated by the Northeast Radio Observatory Corporation, a consortium of 13 educational and research institutions, under agreement with Massachusetts Institute of Technology. Other support is provided under NSF Grant GP-25865 and NASA Grant NGR 22-174-003.

References

Bracewell, R. N.: 1962, 'Radio Astronomy Techniques', in *Handbuch der Physik* **54**, Springer-Verlag, Berlin, p. 42ff.

Haystack Observatory: 15 April 1971, Quarterly Progress Report, Westford, Mass. 01886.

Kopal, Z.: 1966, *An Introduction to the Study of the Moon*, Gordon and Breach, New York, p. 168ff.

Kopal, Z.: April, 1968, Scientific Report No. 2, USAF Contract F6105-2-68-C-0002, Univ. of Manchester, England.

Muller, P. M., and Sjogren, W. L.: 1968 *Science* **161**, 680.

Pettengill, G. H., and Thompson, T. W.: 1968, *Icarus* **8**, 457.

Rogers, A. E. E. and Ingalls, R. P.: 1970, *Radio Sci.* **5**, 524.

Sjogren, W. L., Gotlieb, P., Muller, P. M., and Wollenhaupt, W. R.: 1971 *Science* **175**, 165.

Thompson, T. W., Masursky, H., Shorthill, R. W., Zisk, S. H., and Tyler, G. L.: 1970, *Contribution No. 16*, Lunar Science Institute, Houston, Texas.

Zisk, S. H., Carr, M. H., Masursky, H., Shorthill, R. W., and Thompson, T. W.: 1971, *Science* **173**, 808.